Photocurrent instability of PbS-sensitized TiO_2 electrodes in S^{2-} and SO_3^{2-} solution

Jin Sup Hong [a], Don Sung Choi [a], Man Gu Kang [a],
Donghwan Kim [b], Kang-Jin Kim [a],*

[a] *Division of Chemistry and Molecular Engineering, Korea University, Seoul 136-701, South Korea*
[b] *Division of Material Science and Engineering, Korea University, Seoul 136-701, South Korea*

Abstract

The mechanism of photocurrent decay with time of illumination of PbS-coated TiO_2 (PbS/TiO_2) photoelectrochemical cells in S^{2-} and SO_3^{2-} solution was investigated. The photocurrent decay at short circuit can primarily be attributed to the formation of $PbSO_4$ on the surface of PbS, followed by the dissolution of $PbSO_4$ into the aqueous solution. In the presence of pyridine or ethanol in the solution, the J_{sc} decay with time of illumination is reduced due to the suppression of the $PbSO_4$ formation. © 2001 Elsevier Science B.V. All rights reserved.

Keywords: TiO_2; PbS; Photocurrent instability; $PbSO_4$

1. Introduction

Significant progress has been made in solar energy conversion efficiencies using metal complexes coated on a nanocrystalline TiO_2 film, which is prepared to maximize its surface area [1–5]. Grätzel and coworkers reported that TiO_2-electrodes coated with *cis*-di(thiocyanato)-bis(2,2′-bipyridyl-4,4′-dicarboxylate)ruthenium(II) were found to be the most efficient amongst a series of ruthenium-containing dyes [4,6]. To ensure a strong adsorption on the TiO_2 surface, transition metal dyes containing phosphonate groups were synthesized, but they did not allow for a more efficient charge separation at TiO_2 [7–9]. Solar cells based on the ruthenium-dye sensitization may be photoelectrochemically unstable according to recent reports [10,11].

Together with the efforts to synthesize new efficient dyes, the coupling semiconductor particles of nanometer size has received attention as sensitizers to overcome the limited spectral range of TiO_2 arising from its large bandgap ($E_g = 3.2\,\text{eV}$) [9,12,13]. Those semiconductor particles with a smaller bandgap and an energetically high-lying conduction band, such as CdS and PbS, possess some advantages as compared to organic dyes: the absorption ranges are adjustable by controlling the particle size and the surface

properties can be modified to increase the photostability [14–17]. However, in contrast to organic dyes the photochemistry of nanoparticles is yet to be understood. Besides, the photocurrent of the nanocrystalline TiO_2 sensitized by PbS particles was observed to be continuously declining with the time of illumination. Studies on the sensitization by PbS are limited [9,18–21], and photocurrent stability was not studied in detail.

For the purpose of understanding and improving the photocurrent stability of nanocrystalline TiO_2 electrodes sensitized by PbS particles, in this paper we have examined the current–voltage characteristics of the electrodes in an aqueous solution containing S^{2-} and SO_3^{2-} electrolytes. Nanocrystalline TiO_2 electrodes were prepared by sintering spin-coated TiO_2 films, and PbS particles were deposited on the TiO_2 by a chemical bath deposition as described below. The photoelectrochemical measurements were complemented by electrochemical quartz crystal microbalance (EQCM) gravimetry, UV–VIS reflectance spectroscopy, and X-ray diffractometry to characterize the electrode surface. We report that the oxidation of PbS on the surface of the electrode during the photoelectrochemical reaction and annealing leads to the photocurrent instability. It will be shown that the formation and dissolution of $PbSO_4$ from the PbS/TiO_2 electrode surface is suppressed by addition of pyridine, ethanol, or SO_4^{2-} ions in the electrolyte solution, and thus, short circuit photocurrent decay with time of illumination is reduced.

2. Experimental

The nanocrystalline TiO_2 (Degussa P-25) film was prepared according to a published procedure [4] using ITO glass (Samsung Corning Co., $10\,\Omega/\square$). The area of a TiO_2 film electrode exposed to electrolyte solution was typically about $0.1\,cm^2$. PbS particles were coated on the TiO_2 surface by a chemical bath deposition method for 7 min at room temperature from a 100 ml solution consisting of 2.5 ml of 1 M lead acetate, 10 ml of 1 M NaOH, 6 ml of 1 M thiourea, and 2 ml of 1 M triethanolamine [22]. The PbS-coated TiO_2 (hereafter PbS/TiO_2) electrode was washed with 1.0 M HCl solution distilled water and annealed in a quartz tubular furnace for 1 h at 200, 300, and 400°C in air. The PbS/TiO_2 electrode was then illuminated in a two-electrode, one-compartment cell made of Pyrex glass with a Pt counter electrode to obtain the photocurrent–voltage characteristics. The light source was an Oriel 250 W quartz tungsten–halogen lamp. Photocurrent density–voltage (J–V) curves were obtained using a Keithley 236 source-measure unit (SMU). Photocurrent action spectra were measured using an Aminco–Bowman series2 luminescence spectrometer and the SMU. For characterizing the PbS/TiO_2 surface, a Philips X'PERT-MPD X-ray diffractometer, a Physical Electronics PHI-680 Auger nanoprobe, a Hitachi S-4200 SEM, a Cary 5G UV–VIS–NIR spectrophotometer, and an SSI 2803-S X-ray photoelectron spectrometer were utilized. Monochromatic X-ray from Al Kα was used for X-ray photoelectron spectrometry. The spectrometer was calibrated by the use of both gold $4f_{7/2}$ peak and carbon 1s peak. The spectra were fitted by the use of S-prove software. A Perkin-Elmer OPIMA3000XL ICP-AES analyzer was used to measure the amount of Pb in the electrolyte solution. A Hewlett-Packard HP5890GC with HP5988MS was used to confirm the gas produced during annealing. A Seiko EG&G quartz crystal analyzer QCA917 with a EG&G M273 potentiostat/galvanostat was used to measure mass change in ng during the photoelectrochemical process by the use of the equation $\Delta m = -1.099\,\Delta f$, with f in Hz. The thickness of TiO_2 film was determined with a Tencor Alpha Step 200 profilometer.

3. Results and discussion

3.1. Characterization of PbS/TiO$_2$ electrode

The SEM images were obtained to compare the top and the cross-sectional views of the PbS/TiO_2 surface with those of the TiO_2 surface. No size difference between the two samples was apparent, indicating that the PbS particles coated on the TiO_2 surface were smaller than a few nm. From an XRD peak (at $2\theta = 29.7°$) broadening, the average size of PbS particle calculated by the Scherrer equation was indeed about 3 nm. This value agreed with the result of absorption spectroscopy using dependence of bandgap energy from the size of PbS particles [23].
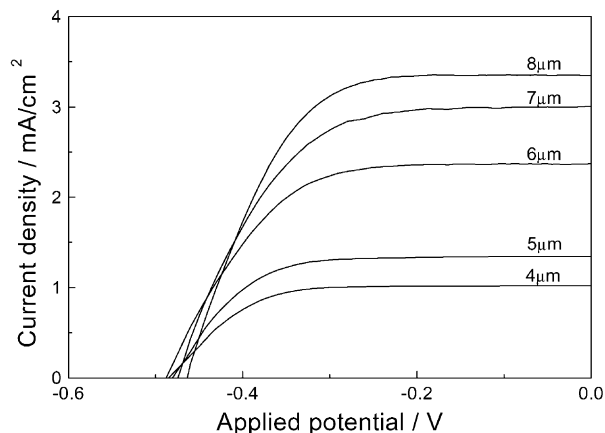

Fig. 1. The J–V curves of PbS/TiO_2 electrodes of various film thickness in $0.4\,M\,Na_2S/0.1\,M\,Na_2SO_3$ aqueous solution. Thickness of the electrodes is indicated above the curves.

Fig. 1 shows a variation of the J–V curves of PbS/TiO_2 electrodes in $0.4\,M\,S^{2-}$ and $0.1\,M\,SO_3^{2-}$ aqueous solution. The electrodes were annealed at 200°C for 1 h. The thickness of the TiO_2 film varied as indicated. The photocurrent was measured at a scan rate of 0.1 V/s under $50\,mW/cm^2$ visible light illumination. The current density of PbS-sensitized TiO_2 film electrodes increased with the increasing the film thickness, due to the increased sensitizer concentration. By the low conductivity of TiO_2 and low transmittance of the PbS/TiO_2 film, the photocurrent density became saturated when the TiO_2 film was thicker than 8 μm. Without the PbS coating, a TiO_2 electrode exhibited almost zero photocurrent over the potential range irrespective of the TiO_2 film thickness under the present condition. Fig. 2 compares the incident photon-to-current conversion efficiency (IPCE) of TiO_2 and PbS/TiO_2 electrodes. The shape of the spectra was in good agreement with the absorption spectra (insets) of the respective electrodes, confirming the sensitization by PbS.
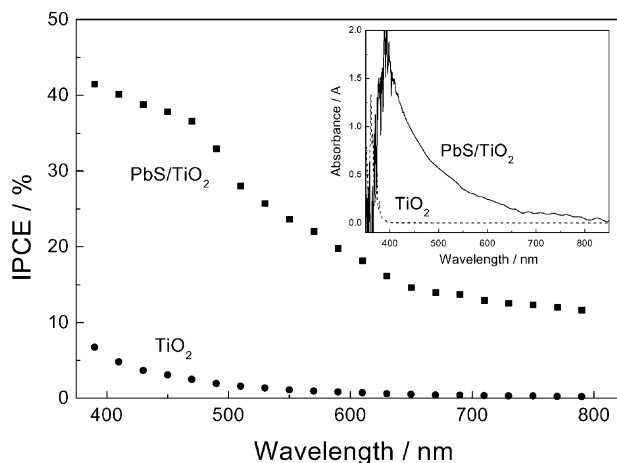

Fig. 2. Photocurrent action spectra and absorption spectra (insets) of TiO_2 and PbS/TiO_2 electrodes. PbS coated on TiO_2 for 8 min. The ordinate scale is expressed as the incident photon to current efficiency (IPCE).

On the other hand, the photogenerated holes in PbS are assumed to react with S^{2-} in the electrolyte solution to result in the formation of S^0 (Eq. (1)), which are subsequently converted by either S^{2-} or $SO_3{}^{2-}$ into $S_2{}^{2-}$ (Eq. (2)) or $S_2O_3{}^{2-}$ (Eq. (3)), respectively.

$$2h^+ + S^{2-} \rightarrow S^0 \tag{1}$$

$$S^0 + S^{2-} \rightarrow S_2{}^{2-} \tag{2}$$

$$S^0 + SO_3{}^{2-} \rightarrow S_2O_3{}^{2-} \tag{3}$$

To ensure a constant photocurrent flow in the outer circuit, both S^{2-} and $S_2O_3{}^{2-}$ produced by the reactions (2) and (3) need to be reduced at the counter electrode (Eqs. (4) and (5)).

$$S_2O_3{}^{2-} + 2e^- \rightarrow SO_3{}^{2-} + S^{2-} \tag{4}$$

$$S_2{}^{2-} + 2e^- \rightarrow 2S^{2-} \tag{5}$$
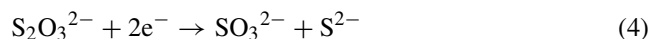
When S^{2-} or $S_2O_3{}^{2-}$ species do not diffuse sufficiently fast to the counter electrode, retardation of the reduction reactions would occur and result in the photocurrent density decrease.

The result shown in Fig. 3 demonstrates that when $S_2O_3{}^{2-}$ was added in the solution the short-circuit photocurrent density (J_{sc}) indeed increases by 11%, but $S_2O_3{}^{2-}$ apparently does not influence the J_{sc} stability. However, in the presence of pyridine or ethanol, hole scavengers, Fig. 3 shows that J_{sc} also decreases but at slower rates. In 1 h, the J_{sc} decreases by 17 and 29% in the presence of pyridine and ethanol, respectively, compared with a 37% decrease in the absence of a hole scavenger.

The J_{sc} of the electrode annealed at 200°C increases by 28% compared with a non-annealed electrode. This enhancement is possibly due to the improved contact between PbS and TiO$_2$ by removing the reactant and solvent molecules. However, at higher temperatures above 300°C a decrease in the J_{sc} is observed. Regardless of the annealing temperature, the J_{sc} showed a similar decay by about 30% in 20 min.
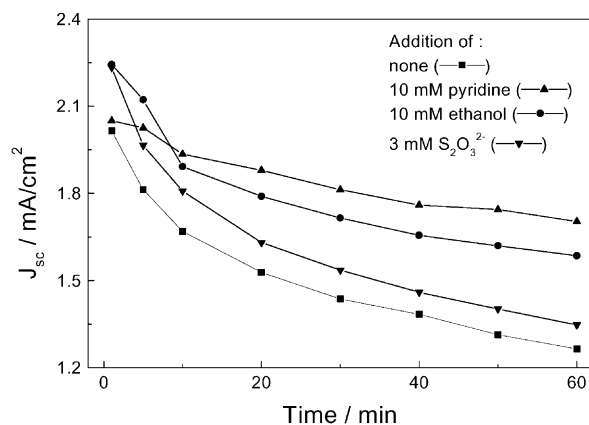
3.2. Oxidation of PbS to PbSO$_4$

From the fact that the hole scavengers such as pyridine and ethanol improve the photocurrent stability, the photocurrent instability possibly arises from corrosion processes involving reactions of photogenerated holes with the PbS on TiO$_2$ or irreversible reactions with the electrolyte [9]. One possibility is insufficient removal of sulfur produced by the reaction of photogenerated holes with S^{2-} in solution (Eq. (1)), and subsequent deposition of sulfur on PbS/TiO$_2$. The deposition of sulfur may increase the barrier for the electron transfer across the electrolyte/PbS interface. Another possibility is a loss of electrode material caused by anodic photocorrosion of PbS/TiO$_2$ and subsequent dissolution of the corrosion product [9,24]. To clarify these possibilities we attempted to examine whether any changes in the PbS/TiO$_2$ electrodes occur during photocurrent measurements. To that end, PbS/TiO$_2$ powder was prepared in the same way as the PbS/TiO$_2$ electrode to remove the possible interference by indium–tin oxide and amorphous glass.

Annealing at and above 200°C turned the dark-brown color of the powder opaque. Similar color change was observed when the powder was exposed to the room light, but wrapping the powder with Al-foil prevented the color change. Upon immersing the annealed powder in a solution containing S^{2-} ions, the dark-brown color was immediately restored. Reflectance spectra recorded with the PbS/TiO$_2$ powder are shown in Fig. 4. The spectra clearly demonstrate that absorption in the visible region diminishes with annealing temperature up to 400°C. Upon immersing the annealed powder in S^{2-} solution, the spectrum (dotted spectrum b) reproduces that of a non-annealed one, which is in agreement with the visual observation.

The XRD patterns indicated that a definite structural change accompanied the color change. Fig. 5 depicts the XRD spectrum of the non-annealed PbS/TiO$_2$ powder showing the presence of both anatase ($2\theta = 25.3, 36.9, 37.8,$
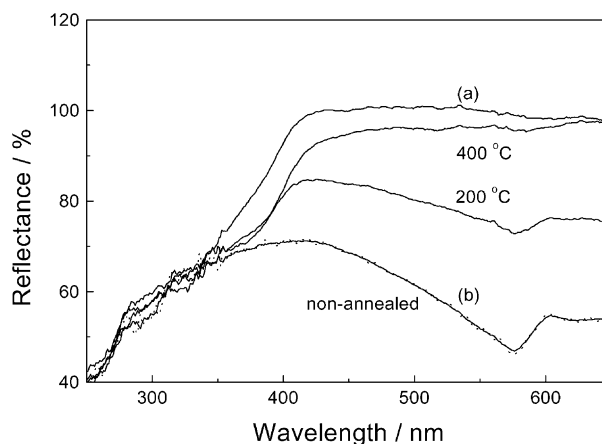
Fig. 3. Photocurrent stabilities of a PbS/TiO$_2$ electrode with addition of 10 mM pyridine, 10 mM ethanol, and 3 mM $S_2O_3{}^{2-}$ in 0.4 M Na$_2$S/0.1 M Na$_2$SO$_3$ aqueous solution.

Fig. 4. Dependence of annealing temperature on reflectance spectra of PbS/TiO$_2$ powder. Data on (a) TiO$_2$ and (b) PbS/TiO$_2$, immersed in S^{2-} solution after annealing at 400°C are included for reference (dotted line).
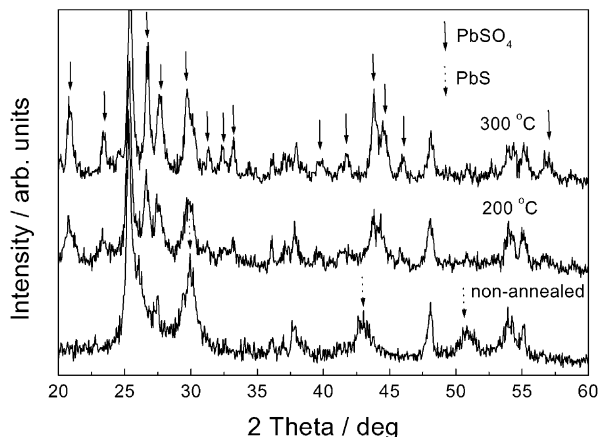
Fig. 5. Variation of XRD pattern by annealing PbS/TiO$_2$ powder. Arrows indicate the PbSO$_4$ peaks and PbS peaks.

Fig. 6. Frequency change of a PbS/TiO$_2$ electrode in 0.4 M Na$_2$S/0.1 M Na$_2$SO$_3$ aqueous solution with time of illumination against applied potential scanned at 100 mV/s.

38.6, 48.0, 53.9, and 55.1°) and rutile phases (2θ = 27.4, 36.1, 39.2, 41.2, 44.1, 54.3, and 56.6°) along with PbS (dotted arrows). Annealing the powder sample develops new peaks indicated with arrows. Some peaks, which were originated from TiO$_2$ or overlapped each other, are not labeled. By comparing newly developed peaks for the annealed PbS/TiO$_2$ with the JCPDS card (no. 36-1461) along with the reflectance spectra in Fig. 4, we concluded that the outer layer of the PbS particles transforms into PbSO$_4$ upon annealing. The possibility of the formation of lead oxides was excluded due to the apparent absence of their corresponding XRD peaks. Immersion of the annealed powder samples into S^{2-} solution gave an identical XRD pattern with the non-annealed one, indicating that PbS is regenerated upon immersion of the annealed powder into S^{2-} solution. Furthermore, a GC/MS measurement for non-annealed PbS/TiO$_2$ powder showed mass peaks at m/z 48 and m/z 64, both of which are related to the production of SO$_2$ from the non-annealed PbS/TiO$_2$ powder. These results suggest that the powder adsorbs excess sulfide ions, which can be oxidized to SO$_2$ or PbSO$_4$ at an elevated temperature.

3.3. Mass change of PbS/TiO$_2$ electrode

To confirm that the change in the PbS/TiO$_2$ powder also occurred in a PbS/TiO$_2$ electrode, the mass change from the PbS/TiO$_2$ electrode coated on a quartz disk under illumination was measured by an EQCM experiment. Fig. 6, a plot of frequency change versus applied potential, reveals that the PbS/TiO$_2$ electrode loses mass by about 7 ng after six scans for the period of 60 s. Voltage was continuously scanned from −0.5 to 0.0 V and reversed to −0.5 V at 100 mV/s. During one cycle the electrode becomes lighter up to −0.13 V on the reverse scan followed by mass gain till −0.5 V. Deposition of sulfur on PbS due to inefficient removal of the sulfur by S^{2-} or SO$_3$$^{2-}$ ions according to Eqs. (2) or (3) may be responsible for the mass gain. The inefficient removal is caused by the repulsion of S^{2-} and
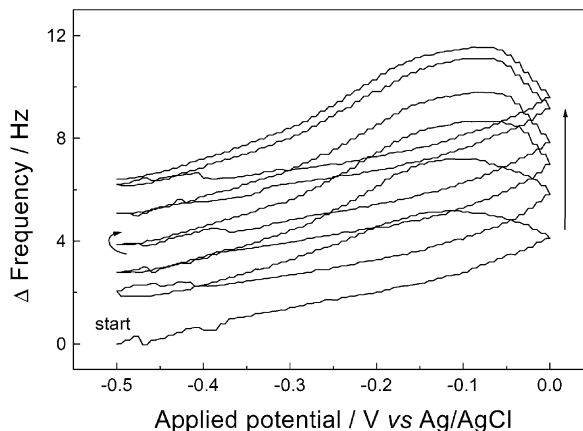
SO$_3$$^{2-}$ ions from the negatively charged electrode below −0.13 V. On the other hand, conversion of PbS into PbSO$_4$ followed by its dissolution may be responsible for the overall mass loss. A ppb level of Pb in the solution after photocurrent measurements, with respect to that in the non-illuminated solution, was detected by an ICP analysis, supporting the dissolution of the photochemically produced PbSO$_4$. In addition, contrary to the annealed PbS/TiO$_2$ powder, the peaks of PbSO$_4$ were not found in the XRD pattern of PbS/TiO$_2$ electrodes after photoelectrochemical measurements. As shown in Fig. 1, the amount of PbS is directly connected with the photocurrent density. Therefore, the gradual decrease in the J_{sc} with time of illumination shown in Fig. 3 can primarily be attributed to the formation and dissolution of PbSO$_4$.

4. Mechanism of photocurrent instability

Based on these observations, the chemical change in the PbS/TiO$_2$ electrode upon illumination can be summarized as follows [9,24]:

$$(PbS_{1+x})_s^{2x-} + (2 + x)O_2 + 2xh^+$$
$$\rightarrow xSO_2 + (PbSO_4)_s \qquad (6)$$
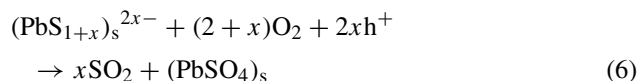
where subscript 's' denotes the PbS/TiO$_2$ surface. However, the interaction between Pb^{2+} and SO$_4$$^{2-}$ on the PbS/TiO$_2$ surface appears to be weak, as evidenced by the immediate restoration of the dark-brown color upon immersion of the discolored PbS/TiO$_2$ powder into the S^{2-} solution. The color restoration can be interpreted as the replacement of SO$_4$$^{2-}$ on the surface with excess S^{2-} in the solution. Therefore, the photocurrent instability at short-circuit with time of illumination can be attributed to the formation of the PbSO$_4$ on the electrode surface and subsequent dissolution of PbSO$_4$ into the aqueous solution. The observed independence of the J_{sc} instability on annealing temperature is a consequence.

Table 1
Atomic concentrations determined by Auger spectroscopy, and positions together with relative intensities of sulfur 2s peak in XPS spectra of the PbS/TiO$_2$ electrode

Electrode	Auger (%)				XPS (eV) of S 2s
	O	Ti	Pb	S	
Non-annealed	60	9	28	3	167 (30),[a] 163 (27), 161 (25), 169 (17)
Discolored[b]	59	9	31	1	171 (25), 169 (75)
Recolored[c]	62	10	24	4	169 (69), 163 (31)

[a] Relative intensity in percent.
[b] Annealed at 300°C for 1 h.
[c] Immersed in S^{2-} solution after annealing at 300 °C for 1 h.

To support the above explanation, Auger spectroscopy and XPS studies were performed on a PbS/TiO$_2$ film electrode. Table 1 lists the data on the atomic concentration of the film collected by Auger spectroscopy and shows that the atomic ratio of sulfur to lead decreases when the electrode is annealed at 300°C and recovers almost the same value after the immersion into the S^{2-} solution. The data on atomic concentration are not corrected for the instrumental sensitivity. Nevertheless, the data on atomic ratios qualitatively confirm the coloring expressed by Eq. (6) and the discoloring arising from the replacement of surface sulfate ions with sulfide ions. Table 1 also includes supporting evidence by XPS that the sulfur 2s peak shifts to a higher binding energy in a discolored electrode than in colored ones, indicating that the oxidation number of sulfur in the discolored electrode is higher compared with the colored one. It is reported that the sulfur 2p peak remains constant on oxidation unlike the sulfur 2s peak [25].

When SO$_4^{2-}$ ions are co-present in the solution, it is expected that the PbSO$_4$ dissolution is suppressed, and thus, the J_{sc} decay with time of illumination is diminished. This notion is confirmed by the result shown in Fig. 7, where the J_{sc} decreases more slowly in the presence of SO$_4^{2-}$ than in the absence of SO$_4^{2-}$.
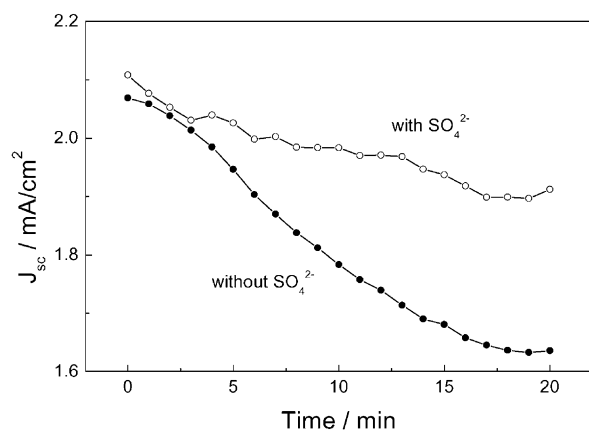

Fig. 7. Comparison of time course of J_{sc} for a PbS/TiO$_2$ electrode in the presence (open circles) with that in the absence (closed circles) of 0.1 M Na$_2$SO$_4$ in 0.4 M Na$_2$S/0.1 M Na$_2$SO$_3$ aqueous solution.

5. Conclusion

Based on the experimental data, it may be concluded that the surface layer of PbS on PbS/TiO$_2$ in S^{2-} and SO$_3^{2-}$ solution is oxidized to PbSO$_4$ under illumination. The formation of PbSO$_4$ in a PbS/TiO$_2$ photoelectrochemical cell slowly deteriorates its photocurrent at short circuit with time of illumination, as a result of loss of the electrode material due to the finite solubility of PbSO$_4$. The addition of pyridine or ethanol, hole scavengers, in the solution reduces the J_{sc} decay with time of illumination due to the suppression of the PbSO$_4$ formation.

References

[1] K. Kalyanasundaram, M. Grätzel, Photosensitization and Photocatalysis Using Inorganic Compounds, Kluwer Academic Publishers, Dordrecht, The Netherlands, 1993, p. 247.
[2] A. Hagfeldt, M. Grätzel, Chem. Rev. 95 (1995) 49.
[3] M.X. Tan, P.E. Laibins, S.T. Nguyen, J.M. Kesselman, C.M. Stanton, N.S. Lewis, in: K.D. Karlin (Ed.), Progress in Inorganic Chemistry, Vol. 41, Wiley, New York, USA, 1994, p. 21.
[4] M.K. Nazeerudin, A. Kay, I. Rodicio, R. Humphry-Baker, E. Müller, P. Liska, N. Vlachopoulos, M. Grätzel, J. Am. Chem. Soc. 115 (1993) 6382.
[5] Y. Tachibana, J.E. Moser, M. Grätzel, D.R. Klug, J.R. Durrant, J. Phys. Chem. 100 (1996) 20056.
[6] B. O'Regan, M. Grätzel, Nature 353 (1991) 737.
[7] P. Bonhôte, J.E. Moser, N. Vlachopoulos, L. Walder, S.M. Zakeeruddin, R. Humphry-Baker, P. Péchy, M. Grätzel, Chem. Commun. (1996) 1163.
[8] P. Péchy, F.P. Rotzinger, M.K. Nazeeruddin, O. Kohle, S.M. Zakeeruddin, R. Humphry-Baker, M. Grätzel, Chem. Commun. (1995) 65.
[9] R. Vogel, P. Hoyer, H.J. Weller, J. Phys. Chem. 98 (1994) 3183.
[10] R. Grünwald, H. Tributsch, J. Phys. Chem. B 101 (1997) 2564.
[11] J.H. Bae, D. Kim, Y.I. Kim, K.J. Kim, Bull. Korean Chem. Soc. 18 (1997) 567.
[12] D.C. Schmelling, K.A. Gray, P.V. Kamat, Environ. Sci. Technol. 30 (1996) 2547.
[13] E. Hao, B. Yang, J. Zhang, X. Zhang, J. Sun, J. Shen, J. Mater. Chem. 8 (1998) 1327.

[14] P.V. Kamat, I. Bedja, S. Hotchandani, L.K. Patterson, J. Phys. Chem. 100 (1996) 4900.

[15] K.R. Gopidas, M. Bohorquez, P.V. Kamat, J. Phys. Chem. 94 (1990) 6435.

[16] B. O'Regan, J. Moser, M. Anderson, M. Grätzel, J. Phys. Chem. 94 (1990) 8720.

[17] J.S. Hong, J.W. Jeong, W.-S. Chae, K.-J. Kim, Bull. Korean Chem. Soc. 20 (1999) 597.

[18] Y. Sun, E. Hao, X. Zhang, B. Yang, J. Shen, L. Chi, H. Fuchs, Langmuir 13 (1997) 5168.

[19] Z.V. Šaponjić, M.I. Ćomor, T. Rajh, J.M. Nedeljković, in: Proceedings of the 20th International Conference on Microelectronics, Vol. 1, 1995, p. 157.

[20] R. Könenkamp, P. Hoyer, A. Wahi, J. Appl. Phys. 79 (1996) 7029.

[21] P. Hoyer, R. Könenkamp, Appl. Phys. Lett. 66 (1995) 349.

[22] R. Suárez, P.K.T. Nair, Solid State Chem. 123 (1996) 296.

[23] Y. Wang, A. Suna, W. Mahler, R. Kasowski, J. Chem. Phys. 87 (1987) 7315.

[24] H. Tributsch, Ber. Bunsenges. Phys. Chem. 81 (1977) 361.

[25] A.N. Woods, R. Buckley, Appl. Surf. Sci. 17 (1984) 401.